EUROPEAN ORGANIZATION FOR NUCLEAR RESEARCH

MEASUREMENT OF THE $(K^+ \to \pi^0\mu^+\nu)/(K^+ \to \pi^0 e^+\nu)$ BRANCHING RATIO*)

J. Heintze, G. Heinzelmann, P. Igo-Kemenes, R. Mundhenke[1],
H. Rieseberg, V. Roberto[2], B. Schürlein[1],
H.W. Siebert, V. Soergel, H. Stelzer[3], K.-P. Streit,
A.H. Walenta[4]

Physikalisches Institut der Universität Heidelberg,
Heidelberg, Germany

and

CERN, Geneva, Switzerland

ABSTRACT

Partial branching ratios $(K^+ \to \pi^0\mu^+\nu)/(K^+ \to \pi^0 e^+\nu)$ have been measured in six lepton momentum bins between 120 and 180 MeV/c. From these, six relations between the form factor slopes λ_+ and λ_0 have been derived. Using the world average value $\lambda_+ = 0.029 \pm 0.003$ and combining the six partial results on λ_0, we obtain $\lambda_0 = 0.019 \pm 0.010$. This value is in agreement with the Callan-Treiman relation and other predictions. Together with recent $K^0_{\ell 3}$ results, it supports the $\Delta I = 1/2$ rule. The agreement of our result with the value of λ_0 obtained from $K_{\mu 3}$ Dalitz-plot studies supports muon-electron universality.

Geneva - 24 June 1977

(Submitted to Physics Letters B)

---

*) Work supported by the Bundesministerium für Forschung und Technologie.

1) Now at IDAS GmbH, D-625 Limburg, Kornmarkt 9, Germany.

2) Now at IFT, Miramare-Trieste, Italy.

3) Now at Gesellschaft für Schwerionenforschung, Darmstadt, Germany.

4) Present address: Brookhaven National Laboratory, Upton, NY, USA.

The branching ratio $R^+ = \Gamma(K^+ \to \pi^0\mu^+\nu)/\Gamma(K^+ \to \pi^0 e^+\nu)$ has been measured in various experiments and the results are known to be rather inconsistent. In view of the importance of this quantity for the determination of the $K_{\ell 3}$ form factors and for the question of muon electron universality, we attempted a new, precise determination of this branching ratio.

Assuming a pure vector coupling, the $K_{\ell 3}$ transition amplitude depends on two form factors, f_+ and f_0, which are usually parametrized as linear functions of q^2, the square of the four-momentum transfer to the leptons:

$$f_{+,0}(q^2) = f_{+,0}(0)\left[1 + \lambda_{+,0}(q^2/m_\pi^2)\right] . \qquad (1)$$

The focal point of interest is the value of λ_0, λ_+ being by now well established. Reviews on the subject, both theoretical and experimental, can be found elsewhere [1-3].

Muon-electron universality implies identical form factors for $K_{\mu 3}$ and K_{e3} decays. Under this assumption the $K_{\mu 3}/K_{e3}$ ratio in a given lepton-momentum interval may be written

$$R = A\left[1 + a\lambda_+ + b\lambda_0 + \mathcal{O}(\lambda_+^2, \lambda_0^2, \lambda_+\lambda_0)\right] . \qquad (2)$$

For the total branching ratio R^+ the kinematical coefficients A, a and b take the values A = 0.645, a = -0.3, and b = 2.2. It can be seen that the measurement of the branching ratio is particularly sensitive to the value of λ_0.

We measured partial $K^+_{\mu 3}/K^+_{e3}$ ratios in six lepton-momentum bins between 120 and 180 MeV/c and, using the well-established value of λ_+, we determined λ_0 from each of these partial branching ratios. The consistency of the results obtained is an indication of the correct treatment of systematic effects. Such effects were expected from the difficulty of identifying muons and positrons from $K^+_{\ell 3}$ decays in the presence of the other decay modes, especially in the presence of pion decays in flight.

The experiment was performed at the short K^+ beam [4] of the CERN PS, and the kaons were required to decay at rest. Concurrently to R^+, the ratios $\Gamma(K^+ \to e^+\nu)/\Gamma(K^+ \to \text{all})$ [5] and $\Gamma(K^+ \to e^+\nu\gamma)/\Gamma(K^+ \to \text{all})$ [6] have been measured.

The layout is shown in Fig. 1. The beam particles were slowed down and about 13000 kaons per PS burst were stopped in a scintillator target (T), consisting of six slabs, each 5 mm thick (i.e. 10 mm in beam direction). The pulse-height distribution in the slabs was used in the analysis to determine the slab in which the kaon stop occurred and to eliminate kaon decays in flight. Charged decay particles were detected by counter hodoscopes H, A, and B. The gas Čerenkov counter (G) [7] served to identify positrons. The momentum of the decay particles was measured in a magnetic spectrometer equipped with drift chambers [8] (D_1 to D_6). The magnet provided a horizontal deflection of 60° at 150 MeV/c. A line width of 4.5 MeV/c FWHM was obtained for the $K^+_{\mu 2}$ decay line (p = 235 MeV/c). The energy of the decay particles was measured in an array of NaI crystals followed by a wall of lead-glass counters (LG). The geometrical acceptance of the spectrometer and the energy-measuring device was about 1%.

The trigger had the following configuration:

$$(K^+ \text{ stop})_{\text{gate}} \cdot (K^+ \text{ decay}) \cdot (e^+ + \mu^+ + \text{monitor}) \ .$$

For a K^+ stop a pulse height of at least 8 MeV was required in one of the target slabs. This had to be followed within 30 nsec by a K^+ decay with the charged decay particle passing through the spectrometer and giving a coincidence H·A·B. Positrons were signalled by the gas Čerenkov counter G and muons selected by the range requirement NaI·$\bar{C}$. The on-line computer selected the triggers with a meaningful track in the drift chambers and counter hodoscopes; it performed a preliminary momentum determination and restricted data recording to the momentum region below the intense $K_{\mu 2}$ and $K_{\pi 2}$ decay lines. A fraction of all decays (1/256) was retained without any restriction to serve as a monitor for the experiment; this sample contained essentially the $K_{\mu 2}$ and $K_{\pi 2}$ decays. The final recording rate was about 4 events per PS burst.

The off-line analysis was restricted to the events in the momentum region from 120 to 180 MeV/c *). Outside this region, pions from $K^+_{\pi 2}$ and $K^+_{\pi 3}$ decays represent a prohibitive background. The sample of e^+ triggers contained, besides the K^+_{e3}

*) Throughout this paper the term "momentum" means the value measured by the spectrometer. This differs from the decay momentum by the amount lost in the target region. Before reaching the spectrometer the decay particles had to traverse, on the average, 1.25 g of matter (carbon equivalent).

decays, only a small amount of events with electron-positron pairs (6%). The sample of μ^+ triggers was composed of $K^+_{\mu 3}$ decays (37%), pion decays in flight (48%), $K^+_{\pi 2}$ decays with a subsequent scattering in the target (11%), $K^+ \to \mu^+\nu\gamma$ decays (2.6%), and K^+_{e3} decays (1.2%).

The $K^+_{\ell 3}$ content of the samples was enriched by the following requirements: (a) Exactly one hit was required in each plane of the chambers D_2 to D_6 and at least one hit in each plane of D_1. (b) No signal was required in the scintillators V_L covering the target in backward direction (see Fig. 1). (c) The reconstructed track was required to hit the NaI array within a fiducial area which excluded the edges of the individual crystals; this was to ensure a pulse height proportional to the energy. (d) It was required that there be no difference between the momentum values deduced from all useful chamber combinations*), and that the vertical track angles, before and after the magnet, could be related to each other. (The correct relations were taken from K^+_{e3} decay tracks.) It was also required that one of the hits in chamber D_1 matched the track defined by D_2 and D_3.

Criteria (a) and (b) eliminated events with more than one charged decay particle; cut (c) ensured that the momentum-energy relation could be used later to separate muons from pions; the combined criterion (d) recognized 95% of the pion decays in flight by their decay kink. In order to minimize any possible biases, the selection criteria (a) to (d) have been applied identically to the μ^+- and e^+-trigger samples.

At this point the remaining events were subdivided into six momentum bins of 10 MeV/c width, and each of the subsamples was treated separately. Figure 2a shows the mass distribution of all events belonging to one of the momentum bins, obtained by combining the measured momentum and energy for each event. It exhibits three clear peaks at the e^+, μ^+ and π^+ masses. Dashed and full lines correspond to e^+- and μ^+-trigger events, respectively. The determination of the number of $K^+_{\mu 3}$ and K^+_{e3} decays was based on the study of these mass distributions.

The detection efficiency for e^+ was nearly 99%: the gas Čerenkov counter tagged about 96% of the positrons. From the remaining 4%, 72% appeared in the

---

*) Useful chamber combinations were: (D_2,D_3,D_4), (D_2,D_3,D_5), (D_2,D_3,D_6), (D_2,D_4,D_5), (D_2,D_4,D_6), (D_3,D_4,D_5), (D_3,D_4,D_6).

μ^+-trigger sample at the e^+ mass (see Fig. 2a), while 28% fired the veto counter C and escaped recording. These numbers were obtained, for each momentum bin, from the sample of tagged positrons. The contamination of the e^+-trigger sample by muons or pions was less than 10^{-3}. To determine $N(K^+_{e3})$, the number of K^+_{e3} decays (Table 1, column 2), the efficiency corrections were applied and the background from pair production was subtracted. The latter was measured by inverting the spectrometer polarity and looking for events with a single e^-. The resulting K^+_{e3} spectrum is shown in Fig. 2b, together with the background from pair production.

To determine the number of $K^+_{\mu 3}$ events we analysed the mass distributions of the μ^+-trigger sample. To this end, we made use of pure μ^+ and π^+ samples of various momenta which had been obtained by slowing down the $K^+_{\mu 2}$ and $K^+_{\pi 2}$ decay particles in copper plates of different thicknesses. Muons were selected by the mass cut $60\ \text{MeV} \leq M < 116\ \text{MeV}$. This sample still contained the following backgrounds: scattered pions due to the finite mass resolution; pion decays in flight which were not eliminated by the track-selection criteria, either because the decay occurred near to the target or because the decay angle was too small to be detected by the chambers; and muons from the decay $K^+ \to \mu^+\nu\gamma$.

The pion background was determined from the measured mass distributions of the pure pion samples mentioned above. The background from pion decays in flight was determined by a careful Monte Carlo analysis. The method was checked by comparing various distributions of the recognized pion decays in the generated and measured data. The contribution of the decay $K^+ \to \mu^+\nu\gamma$ to the various momentum bins was calculated from the formula of Cabibbo [9]. Only internal bremsstrahlung was taken into account since structure-dependent terms are known to make a small contribution [6,10]. The momentum spectra of the $K^+_{\mu 3}$ sample thus obtained and of the various backgrounds after the mass cut are shown in Fig. 2c.

To obtain $N(K^+_{\mu 3})$ in column 3 of Table 1, we corrected for the effect of the mass cut (19% in the lowest momentum bin, 8 to 11% in the others), using the observed mass distributions of the pure muon samples. Another correction (0.4%) took into account muon decay in flight, and muon decay inside the NaI detector with the decay positron hitting the veto counter C. The lowest momentum bin had to be corrected for the muon loss (0.3%) due to the NaI threshold (11 MeV).

The ratio $N(K^+_{\mu 3})/N(K^+_{e3})$ was multiplied by the global correction factor 0.987 ± 0.010, which takes into account slight differences in trigger- and track-reconstruction efficiency for μ^+ and e^+ due to differences in ionization, δ-ray production, and multiple scattering. The corrected μ/e ratios are presented in column 4 of Table 1.

To interpret the measured μ/e ratios in terms of the form factor slopes λ, we calculated the expected values for various combinations of λ_+ and λ_0. This calculation took into account the energy loss and external bremsstrahlung in the target, the spectrometer resolution, and the radiative corrections. The influence of the acceptance variation was checked and found negligible. Using the radiative corrections of Ginsberg [11], we calculate in the six momentum bins the following values for the coefficients A, a and b, which appear in Eq. (2):

Bin:	1	2	3	4	5	6
A:	0.707,	0.712,	0.713,	0.706,	0.686,	0.650
a:	-0.21,	-0.35,	-0.46,	-0.64,	-0.83,	-1.09
b:	2.20,	2.18	2.16,	2.18,	2.22,	2.30

These values indicate that the partial μ/e ratios depend less strongly on λ_+ than on λ_0. Thus we introduced the world average value $\lambda_+ = 0.029 \pm 0.003$ and determined, from the comparison of the measured and calculated μ/e ratios, the values of λ_0. These values are presented in Table 1, where columns 5 to 7 correspond to different hypotheses on radiative corrections.

There is no recognizable dependence of λ_0 on momentum. This indicates the absence of systematic errors in the background treatment. It is therefore justified to work out the average value of λ_0 over the whole observed momentum interval, taking into consideration that the errors are partly correlated in the various momentum bins. The average values of λ_0 are presented in the last row of Table 1.

Most experimental results are based on the radiative corrections of Ginsberg [11]; thus the value in column 6, $\lambda_0 = 0.019 \pm 0.010$, is to be used for comparison with other experiments. Using Eq. (2), this value yields for the total $K^+_{\mu 3}/K^+_{e3}$ branching ratio

$$R^+ = 0.670 \pm 0.014 .$$

In Table 2 our result is compared with other $K^+_{\ell 3}$ and $K^0_{\ell 3}$ experiments. As the K^0 experiments give consistent results, we quote only combined values. Our branching ratio is in good agreement with that of two other $K^+_{\ell 3}$ counter experiments [13,15] and in disagreement with that of two $K^+_{\ell 3}$ bubble-chamber experiments [3,14]. The agreement with the $K^0_{\ell 3}$ experiments supports the $\Delta I = 1/2$ rule.

To describe $K_{\ell 3}$ decays, two approaches are generally put forward. The description which introduces the intermediate states $K^*(1^-;\ 892\ \text{MeV})$ and $\kappa(0^+;\ \simeq 1250\ \text{MeV})$ yields $\lambda_0 \approx 0.014$. The approach based on the Callan-Treiman relation yields the result $\lambda_0 \approx 0.020$. Our result compares favourably with these predictions and helps to clarify the far from satisfactory situation in $K^+_{\ell 3}$ experiments.

The determination of λ_0 from $K_{\mu 3}/K_{e3}$ branching ratios is based on the assumption of muon-electron universality. This is not the case for the determination of λ_0 from $K_{\mu 3}$ Dalitz plot measurements. Thus, muon-electron universality in strangeness changing vector decays can be tested by comparing the value of λ_0 obtained from branching-ratio measurements (λ_0^{br}) with the value taken from Dalitz-plot measurements (λ_0^{Dp}) (columns 3 and 4 of Table 2). To do this we combine our result with those of the two $K^+_{\ell 3}$ counter experiments in Table 2 [13,15] and obtain $\lambda_0^{br} = 0.021 \pm 0.007$. The average value of the $K^+_{\mu 3}$ Dalitz-plot measurements is $\lambda_0^{Dp} = 0 \pm 0.009$. We find $|\lambda_0^{br} - \lambda_0^{Dp}| < 0.036$, with a confidence level (CL) of 90%. Using Eq. (2) we conclude that the $K^+_{\ell 3}$ branching ratio agrees, to within 8%, with the prediction of muon-electron universality.

The above comparison can be performed using the more precise value of λ_0^{Dp} from $K^0_{\mu 3}$ decay ($\lambda_0^{Dp} = 0.020 \pm 0.004$), assuming validity of the $\Delta I = 1/2$ rule. In this case one obtains $|\lambda_0^{br} - \lambda_0^{Dp}| < 0.013$ (90% CL) and an upper limit of 2.9% for the deviation of the $K^+_{\ell 3}$ branching ratio from the prediction of muon-electron universality.

It should be noted that this comparison is based on the radiative corrections of Ginsberg [11].

We wish to thank Mr. E. Ehrbar, Dr. W. Farr, Mr. H. Matsumura and the staff of our workshops for their efficient cooperation. We also thank Mme. M. Jouhet, Mr. L. Bonnefoy and Mr. J. Zimmer for their help during the experiment.

* * *

REFERENCES

[1] L.-M. Chounet et al., Phys. Reports 4C (1972) 199.

[2] G. Donaldson et al., Phys. Rev. D9 (1974) 2960.

[3] H. Braun et al., Nuclear Phys. B89 (1975) 210.

[4] A. Bamberger et al., CERN 72-2 (1972).

[5] J. Heintze et al., Phys. Letters 60B (1976) 302.

[6] J. Heintze et al., Measurement of the $K^+ \to e^+ \nu\gamma$ structure decay, to be published.

[7] J. Heintze et al., Nuclear Instrum. Methods 138 (1976) 641.

[8] A.H. Walenta, Nuclear Instrum. Methods 111 (1973) 467.

[9] N. Cabibbo, Nuovo Cimento 11 (1959) 837.

[10] K.S. Heard et al., Phys. Letters 55B (1975) 324.

[11] E.S. Ginsberg, Phys. Rev. 142 (1966) 1035.

[12] T. Becherrawy, Phys. Rev. D1 (1970) 1452.

[13] D.R. Botterill et al., Phys. Rev. Letters 21 (1968) 766.

[14] D. Haidt et al., Phys. Rev. D3 (1971) 10.

[15] I.H. Chiang et al., Phys. Rev. D6 (1972) 1254.

[16] S. Merlan et al., Phys. Rev. D9 (1974) 107.

[17] P. Beillière et al., Phys. Letters 30B (1969) 202.

[18] G.W. Brandenburg et al., Phys. Rev. D8 (1973) 1978.

[19] G.R. Evans et al., Phys. Rev. D7 (1973) 36.

[20] H.H. Williams et al., Phys. Rev. Letters 33 (1974) 240.

[21] K.F. Albrecht et al., Phys. Letters 48B (1974) 393.

[22] C.D. Buchanan et al., Phys. Rev. D11 (1975) 457.

Table 1

Evaluation and results

(1)	(2)	(3)	(4)	λ_0 $[10^{-3}]$		
				(5)	(6)	(7)
Momentum [MeV/c]	$N(K^+_{e3})$	$N(K^+_{\mu 3})$	$K^+_{\mu 3}/K^+_{e3}$	no RC[a)]	RC of Ref. 11	RC of Ref. 12
120-130	9454 ± 143	7095 ± 231	0.741 ± 0.028	26 ± 17	24 ± 17	17 ± 18
130-140	13039 ± 155	9813 ± 249	0.743 ± 0.022	28 ± 13	24 ± 13	16 ± 14
140-150	15019 ± 155	11243 ± 251	0.739 ± 0.020	29 ± 13	22 ± 13	15 ± 13
150-160	14395 ± 154	10385 ± 234	0.712 ± 0.019	22 ± 13	12 ± 13	6 ± 14
160-170	13228 ± 127	9174 ± 236	0.685 ± 0.020	22 ± 13	9 ± 14	4 ± 14
170-180	11090 ± 111	7489 ± 203	0.666 ± 0.021	39 ± 14	24 ± 14	21 ± 15
120-180	Combined result:			28 ± 10	19 ± 10	13 ± 11

a) RC = radiative correction.

Table 2

Comparison with other measurements

	Experiment	$\Gamma(K_{\mu 3})/\Gamma(K_{e3})$	λ_0^{br} $[10^{-3}]$	λ_0^{Dp} $[10^{-3}]$
K^+	Botterill et al. [13]	0.667 ± 0.017	16 ± 11	
	Haidt et al. [14]	0.596 ± 0.025	-37 ± 22	-12 ± 29
	Chiang et al. [15]	0.698 ± 0.025	38 ± 16	23 ± 14
	Merlan et al. [16]			-18 ± 15
	Braun et al. [3]	0.589 ± 0.020	-41 ± 17	-11 ± 20
	This experiment	0.670 ± 0.014	19 ± 10	
K^0	[17-20]	0.685 ± 0.018	31 ± 13	
	[21, 2, 22]			20 ± 4

Figure captions

Fig. 1 : Experimental layout; a) global view; b) detailed view of the target region; c) target region as seen by the incoming kaons. Detectors: 1 - scintillation counter; $\check{C}$ - plexiglas Čerenkov counter; E, H, A, B, C - scintillator hodoscopes; T - scintillation target; V_L - scintillation veto counter; G - gas Čerenkov counter; L - lead-glass shower counter, not used in the $K^+_{\ell 3}$ BR evaluation; NaI - 18 NaI detector blocks ($17 \times 17 \times 24$ cm^3); LG - 20 lead-glass detector blocks ($17 \times 17 \times 34$ cm^3); D_1 to D_6 - drift chambers, two coordinates each.

Fig. 2 : a) Mass distribution of events in the momentum interval $130 \leq p < 140$ MeV/c.

b) Final K_{e3} momentum spectrum and background ($\times$ 10) from e^+e^- pair production.

c) Composition of the muon sample after the mass cut $60 \leq M < 116$ MeV. The background contributions are scaled up by a factor of five.

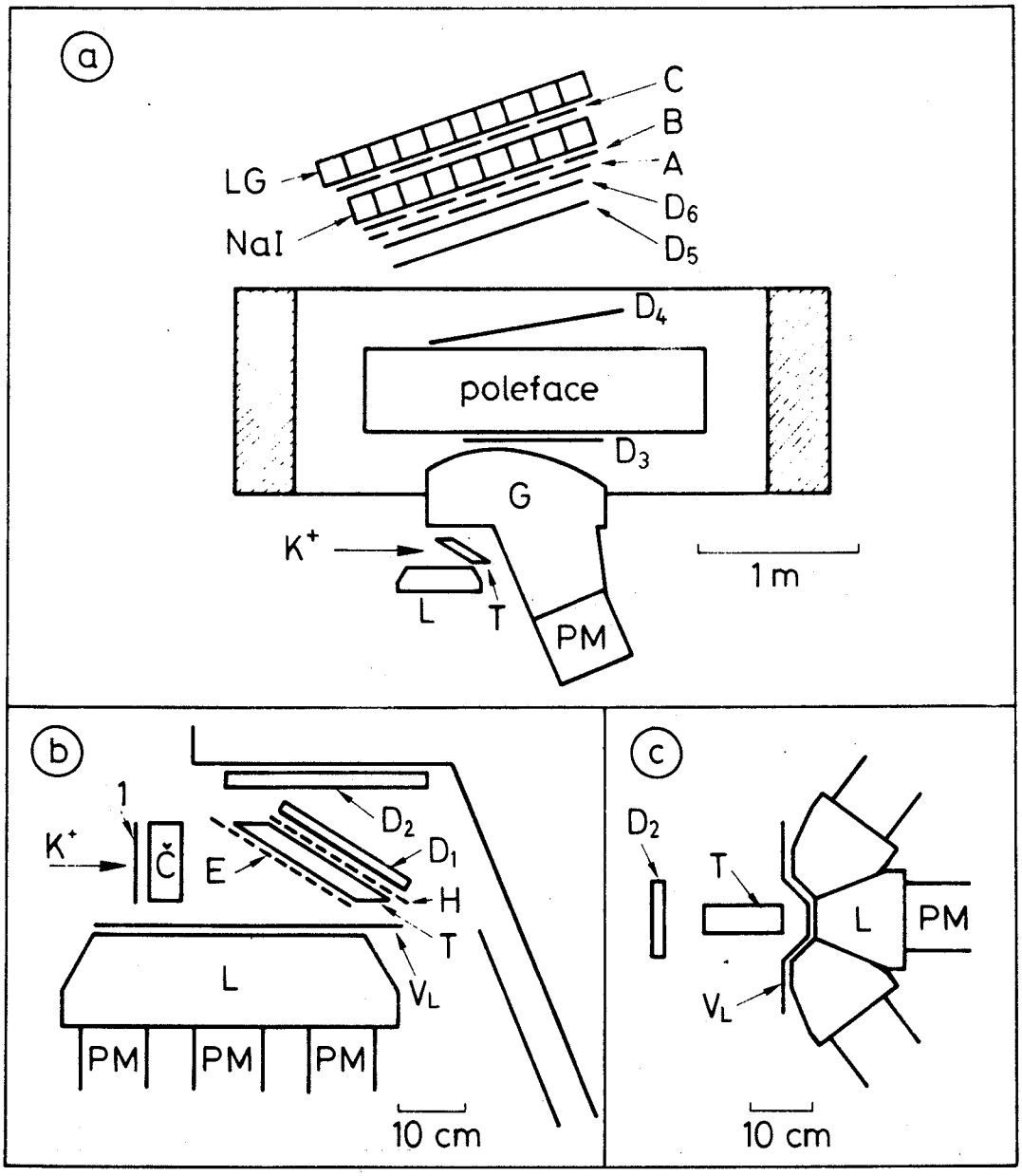
a
C
B
A
LG
NaI
D6
D5
D4
poleface
D3
G
K+
L
T
PM
1 m
b
1
K+
Č
E
D2
D1
H
T
L
VL
PM
PM
PM
10 cm
c
D2
T
L
PM
VL
10 cm

Fig. 1

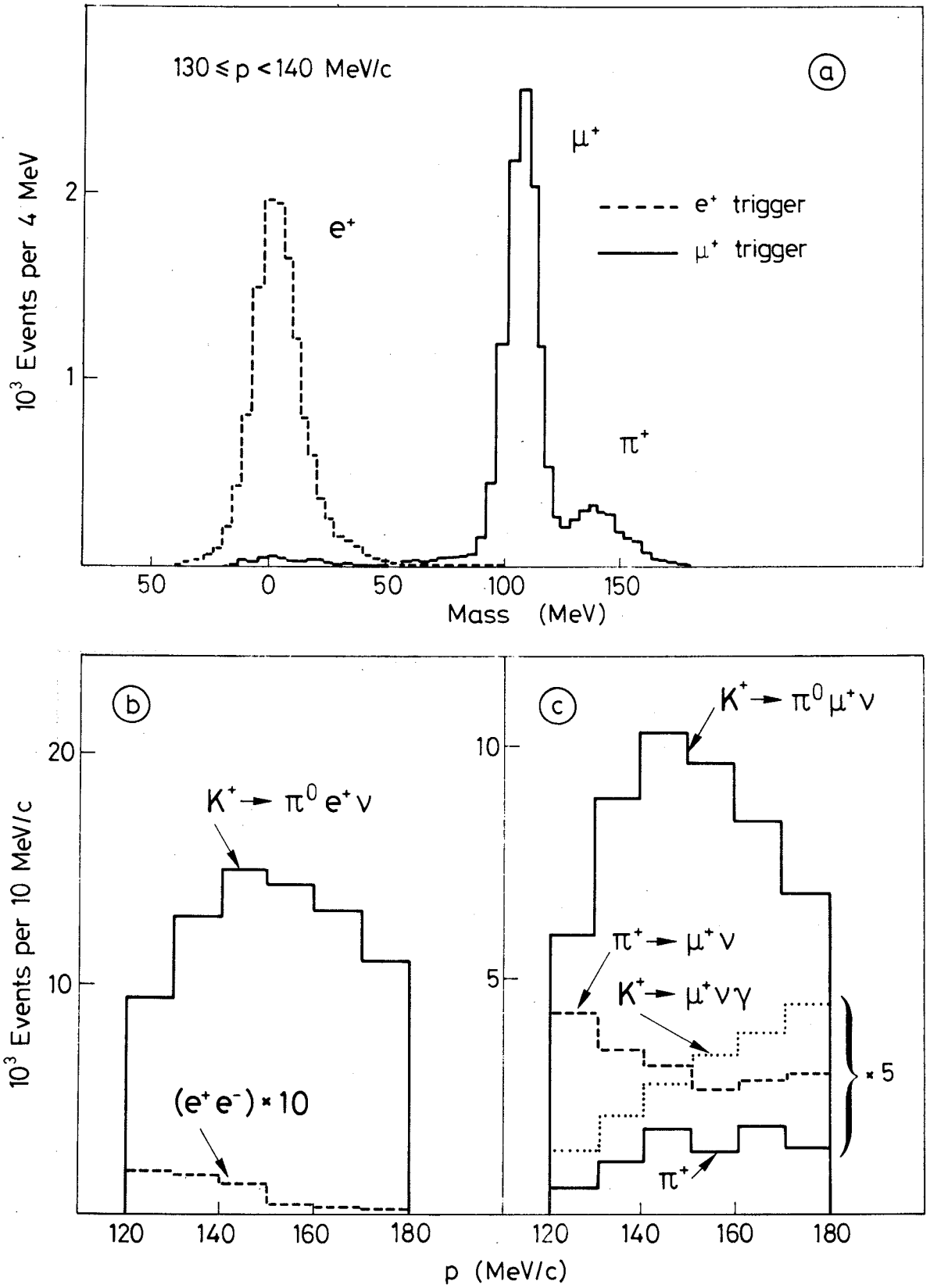
130 ≤ p < 140 MeV/c
a
μ+
e+
π+
e+ trigger
μ+ trigger
10³ Events per 4 MeV
Mass (MeV)
b
K+ → π0 e+ ν
(e+ e−) × 10
c
K+ → π0 μ+ ν
π+ → μ+ ν
K+ → μ+ ν γ
× 5
10³ Events per 10 MeV/c
p (MeV/c)

Fig. 2